

# The dimensions of deep-layer soil desiccation and its impact on xylem hydraulic conductivity in dryland tree plantations

Nana He<sup>1</sup>, Xiaodong Gao<sup>2,3,4\*</sup>, Dagang Guo<sup>1</sup>, Yabiao Wu<sup>1</sup>, Dong Ge<sup>1</sup>, Lianhao Zhao<sup>2</sup>, Lei Tian<sup>5</sup>, Xining Zhao<sup>2,3,4</sup>

5 <sup>1</sup>College of Water Resources and Architectural Engineering, Northwest A&F University, 712100 Yangling, Shaanxi Province, China

<sup>2</sup>Institute of Soil and Water Conservation, Chinese Academy of Science & Ministry of Water Resources, 712100, Yangling, Shaanxi Province, China

<sup>3</sup>Institute of Soil and Water Conservation, Northwest A&F University, 712100, Yangling, Shaanxi Province, China

10 <sup>4</sup>National Engineering Research Center of Water Saving and Irrigation Technology at Yangling, 712100, Shaanxi Province, China

<sup>5</sup>Institute of Green Development Yellow River Drainage Basin, Lanzhou University, 730000, Lanzhou, Gansu Province, China

*Correspondence to:* Xiaodong Gao (gao\_xiaodong@nwafu.edu.cn)

**Abstract.** In water-limited areas, planted trees can extract substantial amounts of soil water from deep layers (>200 cm) to meet their high-water demand, resulting in deep soil desiccation, which influences not only regional water cycling but also the sustainability of trees *per se* in drylands. However, the specific dimensions of deep soil desiccation in relation to both the soil moisture limitation and the maximum root water uptake (RWU) depth are still not well determined. Whether the dimensions depend on tree species and how they will affect tree's xylem hydraulic conductivity are also unclear, restricting our ability to predict the fate of dryland tree plantations. Therefore, we studied the spatiotemporal distribution of deep soil moisture deficit (DSMD) for two typical planted trees, apple (*Malus pumila* Mill.) and black locust (*Robinia pseudoacacia* L.), based on published data and multiple field samplings on China's Loess Plateau. The results indicated that the lowest deep soil moisture (DSM, grav-%) occurred under the planted trees aged 24-28 years at all sites. The lowest DSMD varied around -0.6, which was close to the DSMD at the permanent wilting point (*PWP*, grav-%), regardless of tree species and site, although shallow (<200 cm) soil moisture was not reduced to the point of limitation. This suggests that *PWP* is a reliable indicator of the moisture limitation of deep-layer soil desiccation for the tree species examined. The corresponding depth of soil moisture use reached 18.0-22.0 m for these old planted trees at different sites while it was more than 25 m for *R. pseudoacacia* in the drier site of Mizhi. Furthermore, the mean values of native percentage loss of hydraulic conductivity of planted trees' branches xylem reached 74.9-96.5% in the plantations sampled in this study, indicating that tree mortality may occur. The findings help predict the sustainability of planted trees in semiarid regions with thick vadose zone.

## 30 1 Introduction

Worldwide, tree planting is extensively advocated as a nature-based solution to facilitate the realization of Sustainable Development Goals (Griscom et al., 2020). China's Loess Plateau (LOP), the greatest loess deposits in the world with a

thickness of 30-200 m loess (Shao et al., 2018), has been one of the most active regions for tree planting during the last four decades, with the aim of controlling severe soil erosion and improving rural lives (Fu et al., 2016). Many trees of a variety of species (mostly exotic) have been planted during implementation of two large ecological projects: the Three-North Shelter Forest Program and the Grain-For-Green Program (Cao et al., 2021). So far, the area of tree plantations on the LOP has reached 7.47 million ha; the vegetation cover for this region increased from 31.6% in 1999 to 65.0% in 2017 (official data from the National Forestry and Grassland Administration, <http://www.forestry.gov.cn>). As a result, a number of ecosystem services, including soil and water conservation, have been greatly improved on the LOP (Fu et al., 2016; Gao et al., 2021). In fact, the success of ecological restoration through tree planting on the LOP largely depends on the presence of an abundant “soil reservoir” deposited in deep loess deposits (200-2000 cm) (Zhu, 2006).

However, inappropriate tree planting in drylands can incur other ecological issues, such as soil desiccation due to excessive water consumption (Wang et al., 2010; Jia et al., 2017; Wu et al., 2021), preventing the sustainable development of revegetation and may even result in tree mortality (Breshears et al., 2013; Choat et al., 2018; Stovall et al., 2019). Considerable studies have shown that planted trees extract substantial deep-layer soil moisture (DSM, grav-%) by developing deep roots to maintain their normal growth on the LOP (e.g., Gao et al., 2018; Su and Shanguan, 2019; Shi et al., 2021; Wang et al., 2023). However, continuous use of DSM over several years leads to severe soil desiccation (Wang et al., 2011; Gao et al., 2018; Tao et al., 2021), because DSM below 200 cm is hardly recharged by precipitation under tree plantations. In fact, deep-layer soil desiccation under tree plantations varies in degrees depending on tree age and local climate (Fang et al., 2016; Jia et al., 2017). Although soil desiccation has been widely reported in the above citations, the knowledge about variations in the lowest moisture of deep-layer soil desiccation that limits growth (hereafter “moisture limitation”) and/or the maximum depth from which trees can extract water (hereafter “maximum RWU depth”) for different species and in different climatic regions remains limited. This is critical to estimate the amount of available soil water storage in deep soil and to predict the fate of planted trees based on soil water availability. Currently, permanent wilting point (*PWP*, grav-%) is often used to represent the lowest limitation of soil moisture available to plants according to the definition of available water capacity (Tormena et al., 2017). However, the *PWP* determined in the lab and/or field is often related to annual crops rather than perennial mature trees (Lucia et al., 2020). In the literature, it is mainly estimated based on overall soil properties and uses soil moisture at -15 bar as the surrogate without considering differences between plant species (Torres et al., 2021). However, a recent synthesis indicated that the lowest soil moisture (moisture limitation) under tree plantations can be lower than the average *PWP* on the LOP (Li et al., 2021a). Therefore, it remains unclear whether the *PWP* is a reliable indicator of the moisture limitation of deep-layer soil desiccation for planted trees.

The occurrence of soil desiccation in deep layers can greatly affect the growth and eco-physiological traits of the planted trees. It has been widely observed that the aboveground growth of planted trees is greatly constrained due to deep soil drying,

resulting in so-called “dwarf aged trees” on the LOP (Hou et al., 1991; Zhu, 2000; Fang et al., 2016). Recently, Li et al. (2021) found that when deep soil below 200 cm is dry, the canopy transpiration of apple trees (*M. pumila*) with a rooting depth beyond 2000 cm is reduced by around 40% relative to that without deep soil desiccation on the LOP. Furthermore, Yang et al. (2022) conducted a deep-soil-and-root-partitioning experiment to quantify the effect of deep-layer (>200 cm) root uptake on the transpiration and physiological features of *M. pumila*. They found that the canopy transpiration and the net photosynthetic rate of *M. pumila* without deep-layer root water uptake was reduced, respectively, by 36% and 20% on average, compared with the trees with deep roots in a semiarid site on the LOP. Moreover, resistance of the xylem against embolism increases with a decrease in water availability, leading to a reduction in xylem hydraulic conductivity and even hydraulic failure of European beech (Schuldt et al., 2016; Stojnic et al., 2018). The effect of deep-layer soil desiccation on xylem hydraulic conductivity of planted trees, however, is still unclear, particularly in relation to the two dimensions.

To address the gaps, we built a dataset, including 11980 observations of 258 soil profiles from 34 peer-reviewed publications and 4200 own observations of 72 soil profiles in-situ sampling across the LOP. The main objectives of this study were (i) to identify the moisture limitation and the maximum RWU depth for different tree species and the influencing factors, and (ii) to explore their impact on xylem hydraulic conductivity of planted trees in different climatic regions on the LOP. Our hypotheses were that the moisture limitation and the maximum RWU depth under influence of deep-layer soil desiccation depend on tree species, as they differ in drought-resistance, which is based on their water-use strategy under drought stress (Gessler et al., 2020). Because drought stress causes the formation of gas emboli and blockage of xylem conduits in woody plants, leading to a sharp decrease in xylem hydraulic conductivity (Gauthey et al., 2021), therefore, we also assume that the xylem hydraulic conductivity of planted trees varies among tree species and sites, as the sites represent gradients in aridity.

## 2 Materials and methods

### 2.1 Data compilation

#### 2.1.1 Data sources

Peer-reviewed research papers, published between 1999 and 2021 were extracted from the Web of Science (United States) and CNKI (China Knowledge Resource Integrated Database, China; 2000-2021) using the search terms (“Loess plateau” OR “Loess hilly region”) AND (“artificial forest” OR “afforestation” OR “plantation”) AND (“soil moisture” OR “soil water content” OR “soil water deficit”). To avoid bias in the literature selection, the following criteria were set to filter 718 articles obtained:

- (1) Soil profiles for moisture extraction under deep-rooted artificial forests must exceed a depth of 500 cm at dense sampling intervals ( $\leq 100$  cm). The reason for the criterion is that the 0-200 cm soil layer is greatly affected by rainfall, while the phenomenon of 200-500 cm dry soil layer is common (Jia et al., 2020). Therefore, we considered

data from a sampling depth greater than 500 cm in this study to explore the state of DSM.

- 95 (2) Soil moisture was the gravimetric or volumetric moisture content measured by drying methods or moisture sensors. The volumetric moisture content was uniformly converted to gravimetric moisture content by means of the average soil bulk density in each study area.
- (3) Experiments with only shrub and grass communities or experiments with irrigation, mulching, additional pruning in addition to regular canopy pruning and/or other measures were excluded.
- 100 (4) Experiments yielded paired data for DSM in *M. pumila* orchards or black locust (*R. pseudoacacia*) forests and that in cropland or grassland (control).
- (5) Location, mean annual precipitation (*MAP*, mm), forest age, and vegetation types were clearly presented.

### 2.1.2 Data extraction and classification

A total of 34 peer-reviewed publications were selected for analysis based on the aforementioned criteria. The original data were either clearly obtained from tables in the selected papers or directly extracted from the intuitive figures in those papers using GetData Graph Digitizer (version 2.24, <http://getdata-graph-digitizer.com>). In total, we retrieved a total of 11980 observations from 258 soil profiles, covering 83 sites across four provinces or municipalities (Fig. 1), and the specific information is shown in Table 1. Soil moisture data were collected at 200 cm intervals, with values averaged when multiple samples were obtained within a 200 cm interval (e.g., with an interval of 20 cm or 10 cm). Soil moisture data for the same stand age collected in different sampling years were analyzed independently to assess the influence of forest age on soil moisture. To avoid random errors, data extracted for the moisture limitation of deep-layer soil desiccation under *M. pumila* in Changwu and Luochuan were divided into tree age range for analysis. Simultaneously, we also collected basic data from each publication, including data source, geographic coordinates (longitude, latitude), *MAP*, tree species, and soil texture. Given the limited published information on DSM in *R. pseudoacacia* forests, we also conducted supplementary experiments to obtain relevant data, as described in Section 2.2.

115

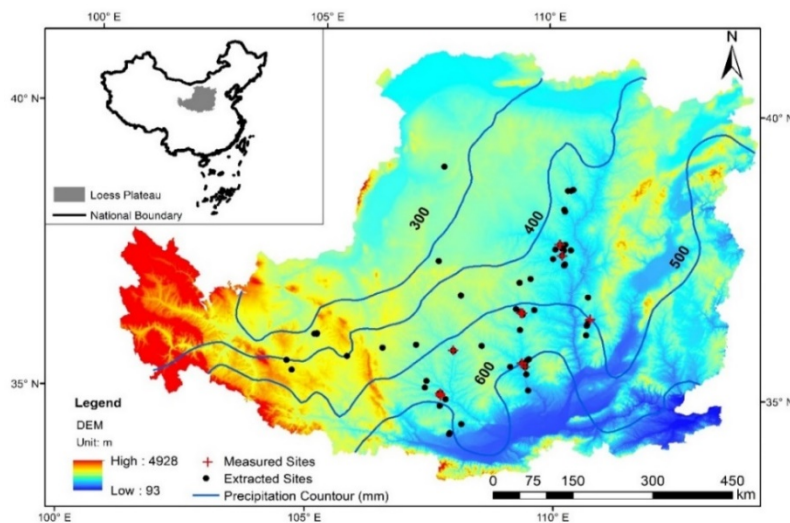


**Figure 1:** Distribution map of sampling sites on the Loess Plateau. The black dots represent the sampling sites extracted from the article, and the red small crosses represent the sampling sites supplemented in the field.

**Table 1.** Sample information used in this study.

Sites	Species	NEP (pair)	NSP (pair)	MAP (mm)	2021-P (mm)	Climate type zone
<b>Luochuan</b>	<b><i>M. pumila</i></b>	24	10	608	957	Semi-humid
Fufeng	<i>M. pumila</i>	1	-	606	-	Semi-humid
Yongshou	<i>R. pseudoacacia</i>	4	-	600	-	Semi-humid
<b>Changwu</b>	<b><i>M. pumila</i></b>	44	8	578	910	Semi-humid
	<b><i>R. pseudoacacia</i></b>	6	10			
Baishui	<i>M. pumila</i>	2	-	577	-	Semi-humid
Jingchuan	<i>M. pumila</i>	1	-	571	-	Semi-humid
Qingcheng	<i>M. pumila</i>	6	-	561	-	Semi-humid
<b>Yan'an</b>	<b><i>M. pumila</i></b>	7	-	530	-	Semi-humid
	<b><i>R. pseudoacacia</i></b>	15	10		704	
Daning	<i>M. pumila</i>	2	-	528	-	Semi-humid
Zichang	<i>M. pumila</i>	1	-	480	-	Semi-arid
	<i>R. pseudoacacia</i>	1	-		-	
Zizhou	<i>M. pumila</i>	1	-	424	-	Semi-arid
<b>Mizhi</b>	<b><i>M. pumila</i></b>	9	10	421	441	Semi-arid
	<b><i>R. pseudoacacia</i></b>	1	10		458	
Total	-	129	58	-	-	-

120 Note: NEP and NSP indicate the number of data pairs from the literature and field sampling, respectively. A data pair refers to the moisture content of a soil profile from plantation and that of a soil profile from cropland/grassland. MAP is the mean annual precipitation, mm; based on MAP, these sites are classified as the semi-arid ( $250 \text{ mm} < \text{MAP} < 500 \text{ mm}$ ) and semi-humid ( $500 \text{ mm} < \text{MAP} < 800 \text{ mm}$ ) climate zone, respectively (Wang et al., 2011). The bold text indicates the supplementary sampling in this study with reference to the existing data, and these are representative plots for the different climatic regions upon which we focused.

## 125 2.2 Data measurement

### 2.2.1 Study area and sampling sites

The LOP covers a total area of 640,000 km<sup>2</sup>, with an elevation range of 200-3000 m. It belongs to the continental monsoon region where annual precipitation ranges from 150 mm in the northwest to 800 mm in the southeast, 55-78% of which falls from June to September (Wang et al., 2011). Fig. 1 and Table 1 show the location of sites from which we collected field data across the entire LOP (34°43'-41°16' N, 100°54'-114°33' E), indicated by the red small crosses and the bold text, respectively. Geographic coordinates (altitude, longitude, and latitude) for each site were obtained using a Global Positioning System (Zhuolin A8, with an accuracy of 1 m).

### 2.2.2 Soil moisture content

135 The sampling events for soil moisture was done from April 9 to May 6 2022 (the early growing season of trees on the LOP) under the plantations of *M. pumila* and *R. pseudoacacia* aged 20-30 years as well as under the cropland/grassland as the control

due to the intact DSM below 200 cm. Initially, the sampling depth was set as 0-10 m under different tree plantations; however, it was extended down to 25 m when the DSM reached the moisture limitation under one given aged plantation as well as under the paired control plots (sampling process is shown in the Fig. S1). The information of the trees showing the lowest deep soil moisture deficit at each site sampled in the field is indicated in Table 2. The maximum sampling depth was set as 25 m because previous studies reported the maximum rooting depth less than 25 m on the LOP (Wang et al., 2009; Li et al., 2019). In order to minimize the spatial variability in soil moisture caused by soil properties, the straight-line distance between the planted trees and their controls was controlled at less than 500 m, and the average straight-line distance of the three replicates was shown in Table 2. All soil samples were collected by a hand auger ( $\Phi=6$  cm) at depth interval of 20 cm and 1.5 m horizontal to the trunk of trees; and three trees with similar growth status were selected for each age as repeats. Collecting soil samples in the due north direction of the first tree, a clockwise rotation of  $120^\circ$  around the second tree from the due north direction was used as the second sampling point, and a clockwise rotation of  $240^\circ$  around the third tree from the due north direction was used as the third sampling point. Soil samples without roots were put into an aluminum specimen box and used to measure the gravimetric moisture content (grav-%), which was determined by drying method at  $105^\circ\text{C}$  for constant weight. A total of 4200 soil moisture data were collected at 72 soil profiles. Three repeats of soil moisture data under one given tree plantation were averaged when analyzing the moisture limitation and the maximum RWU depth under plantations to eliminate the effect of different sampling directions. Moreover, the soil sampling under all tree plantations was done once because the temporal variation of DSM below 200 cm under tree plantations was negligible in one growing season (Fig. S2; Gao et al., 2018; Li et al., 2019).

**Table 2.** Basic information for the trees showing the lowest deep soil moisture deficit at each site sampled in the field.

Sites	Plant species	Longitude	Latitude	Elevation (m)	SD (m)	Stand age (yr)	PH (m)	BD (cm)	DBH (cm)	CD (m)
Mizhi	<i>M. pumila</i>	110°10'22"	37°52'13"	1135.1	430	27	3.5±0.25	5.8±0.53	4.9±0.21	5.73±0.35
	Cropland	110°11'09"	37°52'21"	1139.6		-	-	-	-	-
	<i>R. pseudoacacia</i>	110°13'58"	37°40'08"	1086.2	433	24	9.3±0.40	8.9±0.43	7.3±0.17	5.65±0.75
	Grassland	110°13'46"	37°40'16"	1076.4		-	-	-	-	-
Luochuan	<i>M. pumila</i>	109°21'59"	35°46'44"	1086.9	182	28	2.85±0.35	8.8±0.82	8.1±0.52	4.51±16.7
	Cropland	109°21'58"	35°46'38"	1083.9		-	-	-	-	-
Yan'an	<i>R. pseudoacacia</i>	109°23'22"	36°40'02"	1325.1	412	25	14.35±0.25	9.3±0.19	7.9±0.86	5.81±0.77
	Grassland	109°22'29"	36°40'31"	1333.2		-	-	-	-	-
Changwu	<i>M. pumila</i>	107°41'01"	35°14'12"	1231.7	390	24	4.42±0.25	6.1±0.29	5.4±0.73	4.77±0.13
	Cropland	107°40'43"	35°14'20"	1232.6		-	-	-	-	-
	<i>R. pseudoacacia</i>	107°41'45"	35°12'50"	1215.2	212	28	13.35±0.25	9.4±0.66	8.1±0.51	5.96±0.01
	Grassland	107°42'12"	35°12'36"	1219.4		-	-	-	-	-

Note:  $A\pm B$ , A represents the average of the three replicates of each parameter, and B represents the standard deviation. SD-Average of straight-line distance between three trees and their controls (cropland or grassland); PH-Average plant height; BD-Average basal diameter; DBH-Average diameter at breast height; CD-Average crown diameter.

### 2.2.3 Native percentage loss of hydraulic conductivity

To explore the influence of deep-layer soil desiccation on the native percentage loss of hydraulic conductivity (*NPLC*, %) of  
160 planted trees across different sites, while collecting soil moisture, six current-year branches with 18-20 cm in length and 2-5  
mm in diameter were cut off in the morning from southern crown of *M. pumila* and *R. pseudoacacia* trees at the tree age when  
the plantations reached the moisture limitation; and three trees with similar growth status were selected as repeats for each site.  
Sampled branches were sprayed with water and enclosed in humidified black plastic bags before excising to minimize water  
loss. After bringing these branches to laboratory, we quickly cut 3-5 cm from the middle of the branch under water and  
165 immediately measured xylem hydraulic conductivity of it by using the xylem embolism measurement system (Xylem  
embolism meter, Bronkhorst, Mon-tigny-les-Cormeilles, France). To prevent water spilt from the branch, the initial xylem  
hydraulic conductivity ( $K_{ini}$ ,  $\text{kg s}^{-1} \text{MPa}^{-1}$ ) was measured with  $1 \text{ mmol}\cdot\text{L}^{-1}$   $\text{CaCl}_2$  solution ( $\text{pH} = 6$ ) through a filter with a filter  
aperture of  $0.22 \mu\text{m}$  at a low pressure of 0.5-1.0 kPa. And at a high pressure of 0.2 MPa, the branch was flushed with  $1 \text{ mmol}\cdot\text{L}^{-1}$   
170  $\text{CaCl}_2$  solution until there was no air bubble, then the xylem hydraulic conductivity was determined again at a low pressure  
of 0.5-1.0 kPa and the flushing was repeated until attaining a maximum conductivity ( $K_{max}$ ,  $\text{kg s}^{-1} \text{MPa}^{-1}$ ). The *NPLC* was  
calculated by,

$$NPLC = \left( 1 - \frac{K_{ini}}{K_{max}} \right) \times 100 \quad (1)$$

#### 2.2.4 Basic parameters of plantation

To accurately target the sample plantation, tree age was determined by using the plant growth cones (Haglof, CO300-52,  
175 Sweden) before sampling, and the crown diameter, basal diameter and diameter at breast height were measured with a tape  
(Table 2). The sampling of tree's root was carried out simultaneously with soil moisture sampling, and soil samples with roots  
was stored in a sealed sample bag to minimize the loss of fine roots ( $\leq 2 \text{ mm}$ ), and then gently rinsed in a 100 meshes sieve,  
removing residual roots from the sieve with tweezers. Each fine root sample was dried at  $65^\circ\text{C}$  to constant weight and weighed  
using an electronic balance with a precision of 0.0001 g to determine root dry weight. Finally, the fine root dry weight density  
180 ( $\text{g m}^{-3}$ ) was calculated using the formula given by Zhao et al. (2022).

#### 2.2.5 Soil texture and permanent wilting point

The sampling of soil properties was done simultaneously as soil moisture was sampled, and the data was showed in Table 3.  
Soil samples without root were air-dried, ground, and then passed through a 16 meshes sieve for measuring soil particle  
composition (i.e., clay, silt and sand contents) and soil pH, and through a 100 meshes sieve for determining soil organic carbon  
185 (SOC), respectively. Soil particle composition was determined by laser diffraction using a Mastersizer-2000 Laser Granularity  
Analyzer (Malvern Instruments, Malvern, England) (Wang et al., 2008). Soil pH was determined by the DELTA 320 pH meter.  
SOC was measured by using the potassium dichromate volumetric method (Fu et al., 2010), and soil organic matter was

converted from SOC (Eq. 4). Due to the challenges of collecting undisturbed soil cores within the 10 m profile, soil bulk density and the *PWP* of each site were estimated using the pedo-transfer functions developed by Wang et al. (2012) and Balland et al. (2008) based on the above indicators, as follows,

$$PWP_i = FC_i \left( 1 - \exp \left( \frac{-0.511 \times clay_i - 0.865 \times SOM_i}{FC_i} \right) \right) \quad (2)$$

$$FC_i = 46.481 - 4.757 \times SOC_i - 14.028 \times \log_{10}(clay_i) - 13.991 \times \log_{10}(sand_i) + 42.261 \times \log_{10}(SOC_i) - 11.763 \times sand_i^{-1} + 19.198 \times SOC_i^{-1} - 5.448 \times BD_i + 0.044 \times SOC_i^2 + 1.975 \times BD_i \times SOC_i \quad (3)$$

$$SOM_i = SOC_i \times 1.724 \quad (4)$$

$$BD_i = 1.8284 + 0.0429 \times \log_{10}(clay_i) + 0.0205 \times clay_i^{0.5} - 0.0125 \times \cos(clay_i) - 0.0061 \times silt_i + 0.0001 \times silt_i \times SG - 0.0098 \times SG - 0.0071 \times SOC_i - 0.0505 \times SOC_i^{0.5} + 0.0002 \times SOC_i^2 \quad (5)$$

where *FC* is field capacity, grav-%; *SOC* and *SOM* are soil carbon content and soil organic matter, g kg<sup>-1</sup>; *BD* is the soil bulk density, g cm<sup>-3</sup>; clay, silt and sand are clay, silt and sand content, %, respectively; *SG* is slope gradient at each sample location, °; and *i* represents the *i*<sub>th</sub> soil depth.

**Table 3.** Basic soil properties of field sampling sites.

Sites	Plant species	Soil type	Clay	Silt	Sand	Soil organic metter (g kg <sup>-1</sup> )	Bulk density (g cm <sup>-3</sup> )	pH
Mizhi	<i>M. pumila</i>	Cultivated loessial soils	15.5	24.3	60.2	2.94	1.28	7.64
	Cropland	Cultivated loessial soils	14.9	25.1	60.0	2.33	1.29	8.44
	<i>R. pseudoacacia</i>	Cultivated loessial soils	13.6	25.0	61.4	3.09	1.28	8.03
	Grassland	Cultivated loessial soils	13.8	25.4	60.8	2.35	1.29	8.36
Luochuan	<i>M. pumila</i>	Dark loessial soils	21.5	37.1	41.4	4.62	1.31	7.54
	Cropland	Dark loessial soils	22.2	38.5	39.3	4.38	1.33	8.17
Yan'an	<i>R. pseudoacacia</i>	Cultivated loessial soils	18.1	33.1	48.8	4.87	1.29	8.07
	Grassland	Cultivated loessial soils	19.6	31.5	48.9	4.43	1.30	8.53
	<i>M. pumila</i>	Dark loessial soils	24.6	38.7	36.7	4.76	1.31	7.35
Changwu	Cropland	Dark loessial soils	25.8	38.7	35.5	4.35	1.32	8.21
	<i>R. pseudoacacia</i>	Dark loessial soils	22.9	38.2	38.9	5.01	1.29	7.96
	Grassland	Dark loessial soils	22.7	38.4	38.9	4.26	1.31	8.23

Note: Sampling depth of basic soil properties, including soil particles (which was divided into clay (<0.002 mm, %), silt (0.002~0.02 mm, %) and sand (0.02~2 mm, %) according to the international soil particle classification standard), soil organic carbon (g kg<sup>-1</sup>), and pH was 10 m for different plant species, and the average values of these parameters on different soil layers are presented here. The soil bulk density presents the average value of 1 m soil profile.

### 2.2.6 Meteorological parameters

The precipitation, air temperature, and relative humidity of different sites were from the European Centre for Medium-Range Weather Forecasts ERA5-Land reanalysis (hereafter ERA5-Land) data, and the accuracy of which has been verified by Araújo et al. (2022). Based on the above meteorological data, vapor pressure deficit (*VPD*, kPa) was calculated by using Eq.6.



$$VPD = 0.61078 \times e^{\frac{17.27 \times T_a}{T_a + 237.3}} \times (1 - RH) \quad (6)$$

where  $T_a$  is air temperature, °C; and  $RH$  is relative humidity, %.

## 2.3 Data analysis

### 2.3.1 Meta-analysis

In a traditional meta-analysis, the mean values of the treatment and control with their standard deviations or standard errors are extracted from the publications. However, most published papers selected for this study reported their mean values without standard deviations. To maximize the number of observations, the following unweighted meta-analysis approach was adopted (Li et al., 2021b).

$$RR = Ln(X_e / X_c) \quad (7)$$

where response ratio ( $RR$ ) is a unit-free index with positive and negative values indicating either increasing or decreasing soil moisture in response to planted trees' growth.  $X_e$  and  $X_c$  are values of soil moisture under trees and controls for each study, respectively. The soil depth interval analyzed was 200 cm as mentioned in Section 2.1.2. We use a 95% confidence interval (95% CI) to test the statistical difference between the  $RR$  of soil moisture and zero (Deng et al., 2016), the calculation method

of 95% CI showed as Eqs. 8 and 9,

$$SE_{total} = \sqrt{\frac{V_s}{N}} \quad (8)$$

$$95\% CI = 1.96 \times SE_{total} \quad (9)$$

where  $SE_{total}$  is the standard error of  $RR$ , and  $V_s$  and  $N$  are the variances of  $RR$  and the number of observations, respectively. In this study, the statistical difference between the  $RR$  of soil moisture and zero was considered significant if the 95% CI did not include zero, and the differences were not considered significant if the 95% CI include zero.

### 2.3.2 Quantitative index for moisture limitation of soil desiccation

The effect of different deep-rooted planted trees' RWU on soil moisture was expressed as soil moisture deficit, which is the relative difference in soil moisture for given trees and adjacent cropland/grassland. Because root distribution of the latter is too shallow (<2 m) to influence the change of DSM (Gao et al., 2014; Zhu et al., 2016; Gao et al., 2022), the soil moisture of grassland/farmland measured simultaneously with that of plantation can be used as background value to eliminate the influence of climate difference. The soil moisture deficit in the  $k$ th layer of the  $j$ th plantations calculation method as shown in Eq. 10. And the soil moisture deficit of the soil layer below 2 m is the deep soil moisture deficit (DSMD). In order to compare the difference between the DSMD of plantations and their  $PWP$ , the soil moisture deficit corresponding to  $PWP$  in the  $k$ th layer of the  $j$ th plantations along the soil profile was calculated by Eq. 11.

$$SMD_{j,k} = \frac{SMC_{j,k} - SMC_{0,k}}{SMC_{0,k}} \quad (10)$$

$$SMD\_PWP_{j,k} = \frac{PWP_{j,k} - SMC_{0,k}}{SMC_{0,k}} \quad (11)$$

where  $SMC_{j,k}$  and  $PWP_{j,k}$  represent soil moisture content and permanent wilting point in the  $k$ th layer of the  $j$ th plantations, grav-%, respectively;  $SMC_{0,k}$  indicates soil moisture content in the  $k$ th layer of the control (cropland or grassland), grav-%;  $SMD_{j,k}$  and  $SMD\_PWP_{j,k}$  represent the soil moisture deficit corresponding to  $SMC_{j,k}$  and  $PWP_{j,k}$ , respectively.

### 2.3.3 Quantitative index for the maximum RWU depth

The paired sample  $t$ -test in SPSS was used to analyze the significant difference of soil moisture between plantations and their controls. Three duplicate values were taken for each plantation and its control *per* site, and the straight-line distance between them was less than 500 m. If the difference of soil moisture content in the plantation and its' control becomes not statistically significant ( $p > 0.05$ ) at a given layer, it is defined that this depth corresponds to the maximum RWU depth for the planted trees sampled in this study. On the other hand, if it is always statistically significant ( $p < 0.05$ ) along the whole measured profile, this indicates the maximum RWU depth exceeds the measurement depth. A list of all acronyms, the corresponding definitions and units is given in Table 4.

### 2.3.4 Statistical analysis

Redundancy analysis (RDA) was performed to evaluate the contributions of environmental factors to soil moisture deficit and soil moisture using Canoco 5 (Microcomputer Power Ithaca, New York, USA). Least significant difference *post-hoc* tests in SPSS 22.0 software package (SPSS 22.0, SPSS Institute Ltd., USA) was used to analyze the significant differences in *NPLC* of current-year branches of planted trees in different sites (takes the average of six branches as the *NPLC* for *per* tree, and three duplicate trees was treated as independent in statistical analysis),  $\alpha = 0.05$  was considered statistically significant. Origin 2021 software (OriginLab Corporation, USA) was used to draw the figures.

**Table 4.** List of acronyms included in the study, with definition and units.

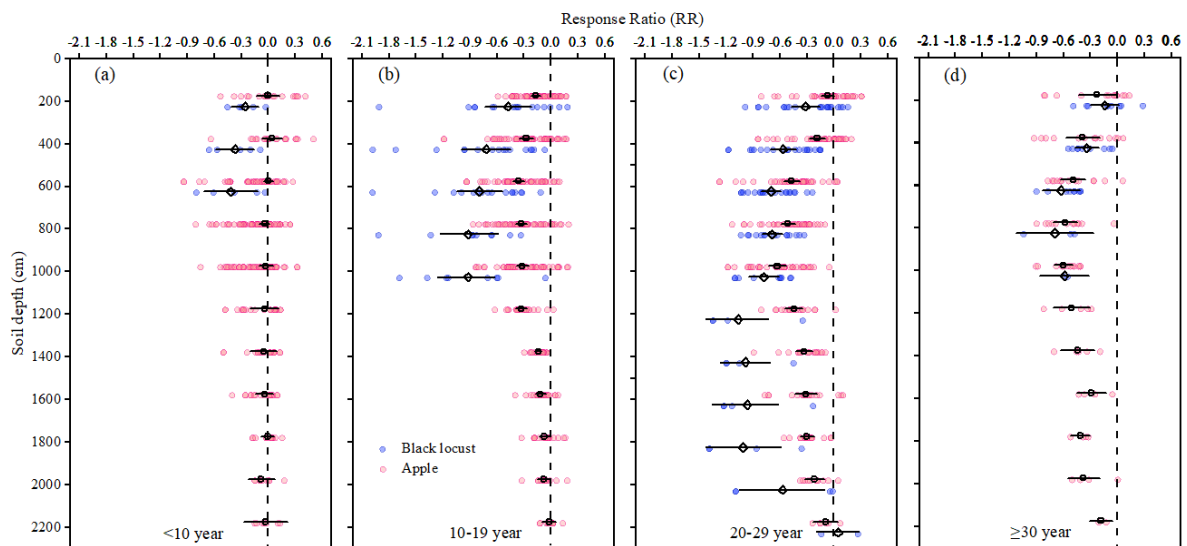
Acronym	definition	Units
Soil properties		
DSMD	Deep soil moisture deficit	-
DSM	Deep soil moisture	grav-%
PWP	permanent wilting point	grav-%
SOC	Soil organic content	g kg <sup>-1</sup>
Research objects		
LOP	China's Loess Plateau	-
<i>M. pumila</i>	Apple trees ( <i>Malus pumila</i> Mill.)	-
<i>R. pseudoacacia</i>	Black locust ( <i>Robinia pseudoacacia</i> L.)	-
SD	Average of straight-line distance between three trees and their controls	m
Plant properties		

PH	Average plant height	m
BD	Average basal diameter	cm
DBH	Average diameter at breast height	cm
CD	Average crown diameter	m
<i>NPLC</i>	Native percentage loss of hydraulic conductivity	%
$K_{ini}$	The initial branch xylem hydraulic conductivity	$\text{kg s}^{-1} \text{MPa}^{-1}$
$K_{max}$	The maximum branch xylem hydraulic conductivity	$\text{kg s}^{-1} \text{MPa}^{-1}$
RWU	Root water uptake	mm
Environmental conditions		
VPD	Vapour pressure deficit	kPa
MAP	mean annual precipitation	mm
Data analysis		
RDA	Redundancy analysis	-
95%CI	95% confidence interval	-

### 3 Results

#### 3.1 Soil moisture under planted trees of the different ages

260 The soil moisture under *M. pumila* orchards and *R. pseudoacacia* forests varied greatly with tree age across the entire soil layer (Fig. 2). As tree age increased, the negative effect of *M. pumila* (0-21 m soil layer) and *R. pseudoacacia* (0-10 m soil layer) growth on DSM initially increased and then stabilized. Specifically, the negative effect value of DSM (4-10 m) under *R. pseudoacacia* forests older 30 years decreased by 17.4% compared with those aged 20-30 years. Therefore, the two plantations had the greatest effect on DSM at the age range of 20-30 years. Consequently, plantations within this age range were considered as the main subjects when analyzing the moisture limitation and the maximum RWU depth under the influence of deep-layer soil desiccation for planted trees in Sections 3.2 and 3.3.



265

**Figure 2:** Mean effect sizes indicating the mean value of response ratio (*RR*, a unit-free index with positive or negative value means soil moisture increases or decreases with the older of plantations) of soil moisture with the age of plantation on the Loess Plateau are divided into: (a) tree age <10 year, (b) 10 year ≤ tree age <20 year, (c) 20 year ≤ tree age <30 year, and (d) tree age ≥ 30 year. The vertical black dotted

lines indicate  $RR=0$ . Blue and red dots, which involves 11980 literature extraction data and 4200 field sampling data, represent black locust (*R. pseudoacacia*) forests and apple orchard  $RR$ s, respectively; diamonds and circles represent the mean  $RR$  of *R. pseudoacacia* and apple (*M. pumila*) orchard, respectively; and the error bars represent 95%CI.

### 3.2 The dimensions of deep-layer soil desiccation for planted trees

The DSM under a given tree species can vary substantially among different years, even at the same age, due to varying annual precipitation. For instance, the DSM of 15-year-old *M. pumila* in Changwu varied greatly across different sampling years (Fig. 3(a)). To account for climate differences between sampling years, we used soil moisture deficit, which was defined as the relative difference in DSM between the given trees and nearby controls. The DSM of control adjacent to the plantation was regarded as the background soil moisture to reflect local annual precipitation because it was not influenced by root water extraction from annual crops with the shallow roots (<2 m). We found that the variation coefficient of DSMD (Fig. 3(b)) was lower than that of DSM; thus, DSMD was used for the following in-depth analyses.

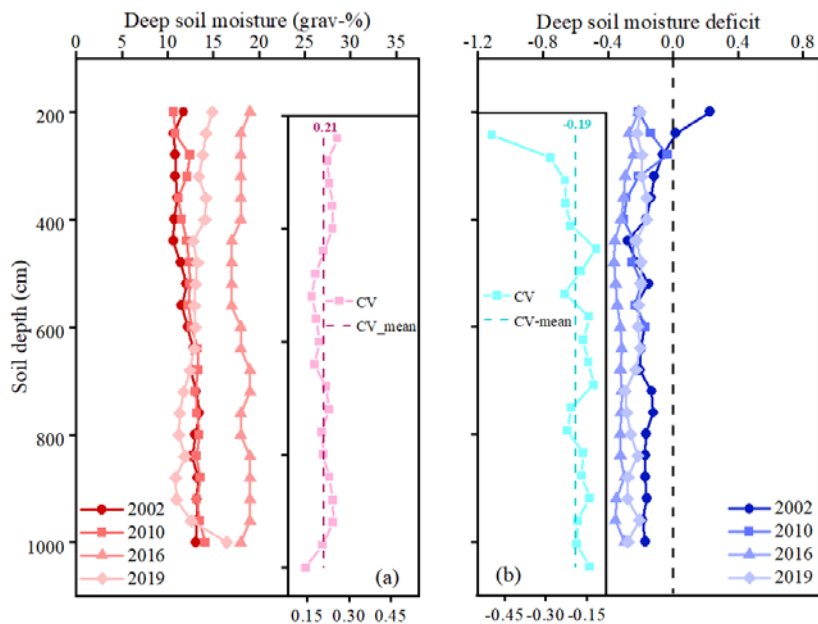


**Figure 3:** Distribution of deep soil moisture (grav-%, (a)) and deep soil moisture deficit (b) of 15-year-old apple (*M. pumila*) orchards in Changwu in 2002, 2010, 2016 and 2019, which is all based on literature extraction data. The variation coefficient (CV) of deep soil moisture and deep soil moisture deficit below 2 m are shown in the small figures, the dashed lines of which represent the mean values of the CV for deep soil moisture and deep soil moisture deficit, respectively.

#### 3.2.1 Moisture limitation of deep-layer soil desiccation

We combined the extracted (Fig. 4(a) and (b)) and measured (Fig. 4(c)-(f)) data to explore the moisture limitation of deep-layer soil desiccation. The DSMD fluctuation in *M. pumila* over 19 years was relatively stable in Changwu, Luochuan and Mizhi (Fig. 4(a)-(c)). Interestingly, with the increase in tree age, the lowest DSMD of *M. pumila* occurred in different sites, and tree age between 24 and 28 years was associated with the lowest DSMD in different sites. After reaching the lowest value, *M. pumila* could no longer extract water from the deep soil. Notably, although there were differences in soil moisture among different sites and tree species (Fig. S3), the lowest value of DSMD in three sites varied around -0.6, which was very close to

the DSMD value corresponding to the local *PWP*. In addition, DSMD of the *R. pseudoacacia* in the Changwu, Yan'an and Mizhi was similar to that of *M. pumila* (Fig. 4(d)-(f)). Namely, the lowest values of DSM consumption were the same as those of *M. pumila* in different sites. This suggests that *PWP* is a reliable indicator of the moisture limitation of deep-layer soil desiccation, regardless of tree species and site. In addition, compared with *M. pumila*, the variation range of DSMD for *R. pseudoacacia* decreased greatly in Changwu and Yan'an.

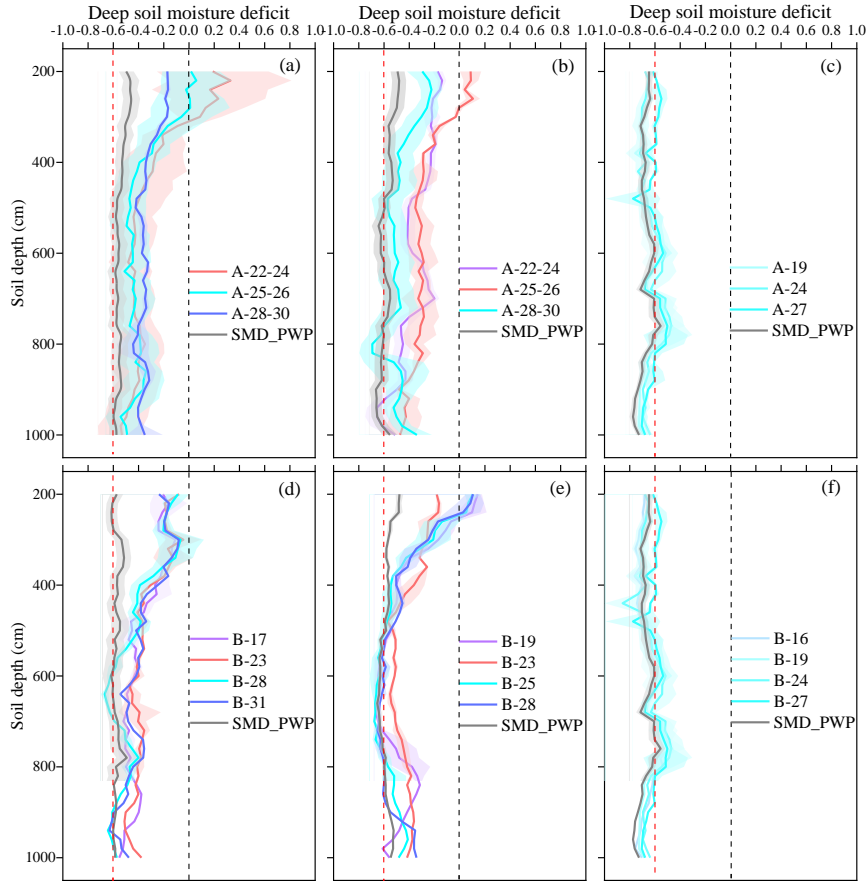


**Figure 4:** Deep soil moisture deficit (DSMD) distribution under apple (*M. pumila*) orchards of different ages in Changwu (a), Luochuan (b) and Mizhi (c); and deep soil moisture deficit under black locust (*R. pseudoacacia*) forests of different ages in Changwu (d), Yan'an (e) and Mizhi (f). The capital letters A and B in the legend represent *M. pumila* and *R. pseudoacacia*, respectively, and the numbers after the letters represent tree age, for example, A-22 represents 22-year-old *M. pumila*. (a) and (b) come from data extracted from literature, while (c)-(f) are both field measured data. In order to reduce the randomness caused by different sampling years and locations between the extracted data, the data for *M. pumila* trees with similar ages in Changwu (a) and Luochuan (b) were combined. The gray line indicates soil moisture deficit at permanent wilting point (SMD\_PWP) in each sampling site, and the red dashed line indicates the soil moisture deficit equal to -0.6. The shaded portion corresponding to each line represents the positive and negative values of the standard deviation.

### 3.2.2 The maximum RWU depth under the influence of deep-layer soil desiccation

Based on the measured and literature data, we analyzed the maximum RWU depth of plantations that reached the moisture limitation of deep-layer soil desiccation in different regions (Fig. 5). With an increase in depth, the soil moisture of plantations was close to or even higher than that of the control in the top 200 cm, except for the *M. pumila* orchards and *R. pseudoacacia* forests in Mizhi. Therefore, we calculated the difference significance of soil moisture between the plantations and control using

the paired sample  $t$ -test, treating the points with no significant ( $p>0.05$ ) soil moisture difference as the maximum RWU depth for the planted trees sampled in this study. In this way, the maximum RWU depth reached 18.0-22.0 m for *M. pumila* orchards at different sites; and 18.4-18.8 m for *R. pseudoacacia* forests in Changwu and Yan'an, whereas it was deeper than 25 m in the drier site of Mizhi.

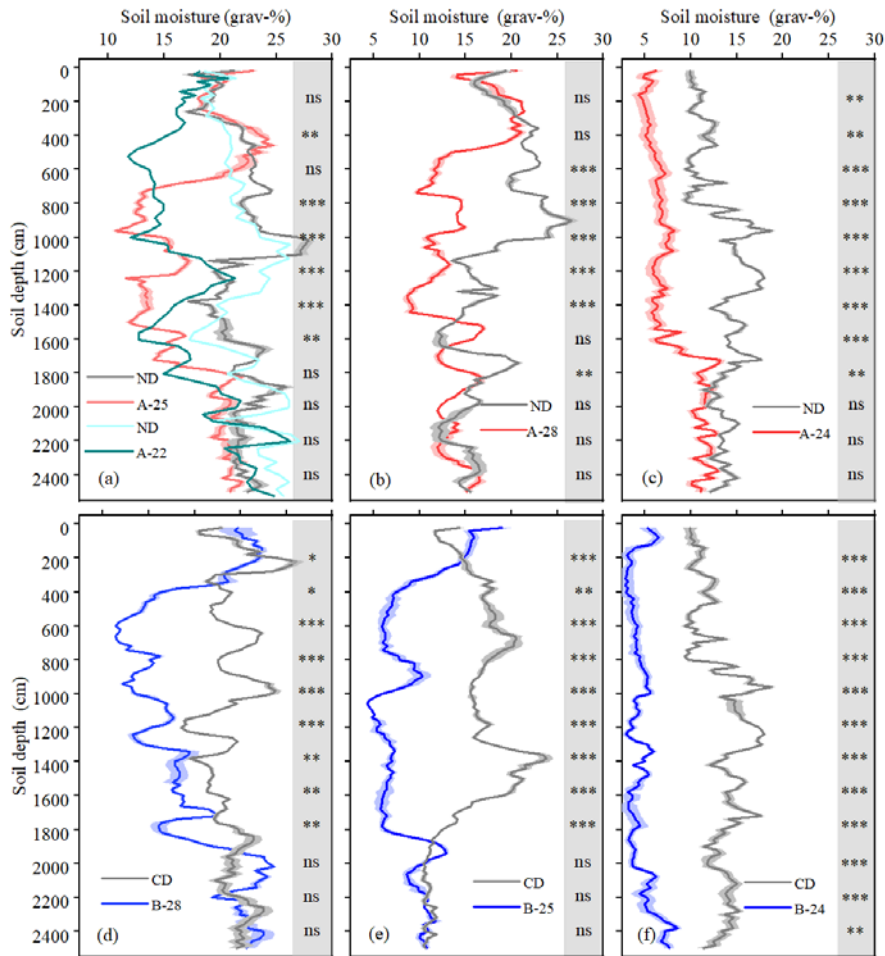


**Figure 5:** Dynamic distribution of maximum water absorption depth after reaching the moisture limitation of deep soil desiccation. The data of 22-year-old apple (*M. pumila*) and cropland (dark green) in (a) belong to literature extraction data, and other data are field measured data. The capital letters A and B in the legend represent *M. pumila* and black locust (*R. pseudoacacia*), respectively, and the numbers after the letters represent tree age, for example, A-22 represents 22-year-old *M. pumila*. (a) and (d) indicate Changwu; (b) and (e) indicate Luochuan and Yan'an, respectively; (c) and (f) indicate Mizhi. Gray line represents soil moisture (grav-%) of grassland (CD) or farmland (ND). \*\*\*, \*\*, \* and ns in the gray bands indicate the significance level of measured data obtained by the paired sample  $t$ -test for  $p<0.001$ ,  $p<0.01$ ,  $p<0.05$  and no significant differences, respectively. The shaded portion corresponding to each line represents the positive and negative values of the standard deviation.

### 3.3 Effect of factors on the dimensions of deep-layer soil desiccation

Based on all extracted and measured data, including soil moisture deficit, soil moisture, soil texture (clay, silt), and fine root dry weight density along with ERA5-Land meteorological data ( $MAP$ , mean annual temperature, relative humidity,  $VPD$ ), we used the RDA to analyze the key factors that determined the moisture limitation and the maximum RWU depth under the influence of deep-layer soil desiccation (Fig. 6). The result indicated that the explanatory variables (soil properties,

meteorological variables and plant characteristic) accounted for 67.7% of the total variation of soil moisture and soil moisture deficit. Soil moisture deficit was significantly ( $p < 0.01$ ) positively correlated with *VPD*, and negatively correlated with clay, silt, relative humidity, mean annual temperature, and *MAP* (Fig. 6(a)). The clay, *VPD*, silt, relative humidity, and fine root dry weight density provided statistically significant ( $p < 0.01$ ) explanations for the distribution of soil moisture deficit and soil moisture (Fig. 6(b)). The clay content determined the lower limit of water that plants could uptake through its adsorption of water molecules. Therefore, soil texture and climatic conditions were the main factors influencing the dimensions of deep-layer soil desiccation in different sites. However, the relationship between *MAP* and soil moisture deficit was not significant, which might be because the *MAP* of each site diminished the differences of precipitation in each sampling year.

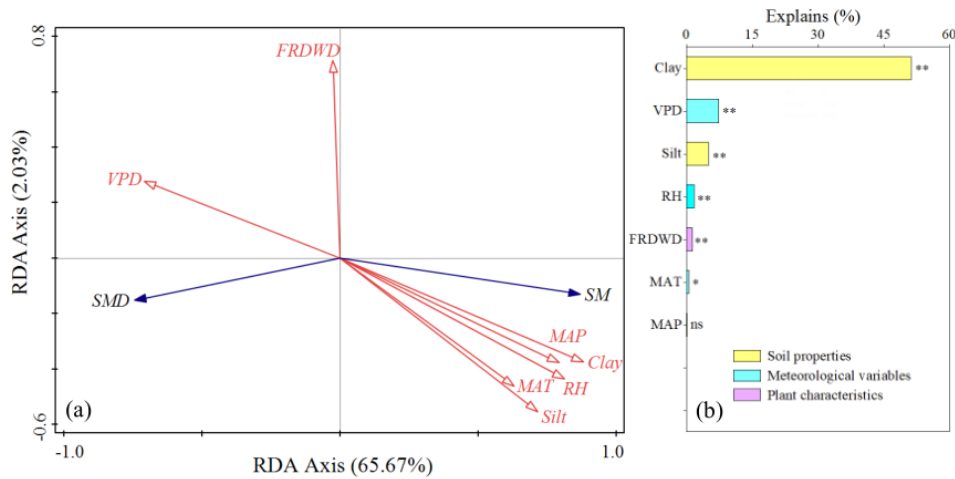


**Figure 6:** (a) the redundancy analysis (RDA) of “response variable (soil moisture deficit (SMD), soil moisture (SM, grav-%)) and environmental factors” is based on literature and field measured data. Descriptors (red arrows) are soil properties (clay and silt), meteorological variables (vapor pressure deficit (*VPD*, kPa), mean annual precipitation (*MAP*, mm), relative humidity (*RH*), and mean annual temperature (*MAT*, °C)), and plant characteristic (fine root dry weight density (*FRDWD*,  $\text{g m}^{-3}$ )). Axis 1 (65.67%,  $p < 0.01$ ) and Axis 2 (2.03%,  $p < 0.01$ ) are shown. (b) explanation provided by of each environmental variable for the response variables. \*\*, \*, and ns following the bar chart indicate that  $p < 0.01$ ,  $p < 0.05$ , and no significant, respectively.

### 3.4 Effect of the dimensions of deep-layer soil desiccation on hydraulic conductivity

To further elucidate how the moisture limitation and the maximum RWU depth under the influence of deep-layer soil desiccation affects the hydraulic conductivity in plants, we explored the variations of hydraulic conductance of branches for different tree species and sites (Fig. 7). Please note that the data used for analysis here were from only the plantations where the moisture limitation and the maximum RWU depth were determined in this study (Figs. 4 and 5). The *NPLC* was higher than 50% for all tree species and sites and exhibited distinct variations between tree species and sites. The *NPLC* ranged from 74.9-96.5% for *R. pseudoacacia* trees and 83.0-92.7% for *M. pumila* trees. Particularly, the *NPLC* of *R. pseudoacacia* trees in Mizhi was significantly higher than that in other sites ( $p < 0.05$ ), indicating that the *R. pseudoacacia* trees in Mizhi had greatest mortality risk in relation to the severe deep-layer soil desiccation.

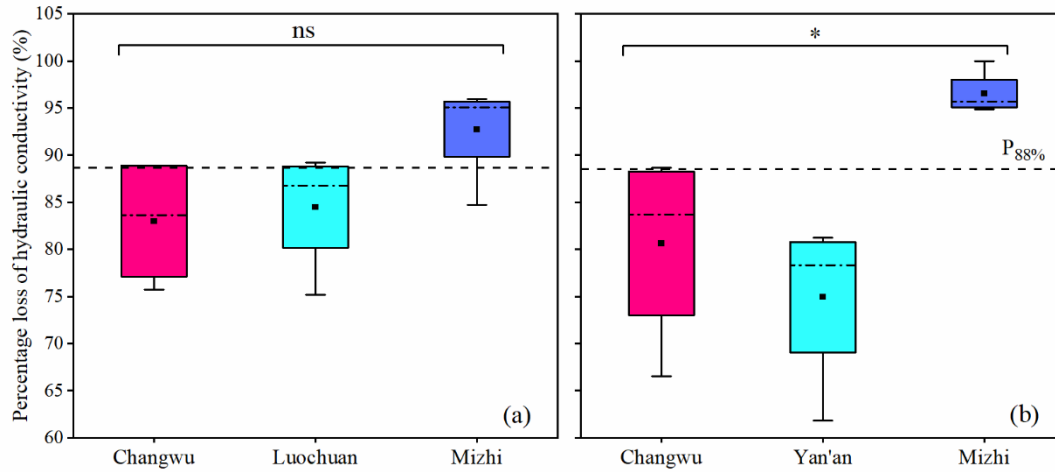


**Figure 7:** Differences in percentage loss of hydraulic conductivity of annual branches of apple (a, *M. pumila*) and black locust (b, *R. pseudoacacia*) measured in different sites (Changwu, Luochuan, Yan'an, and Mizhi). \* and ns indicate that the significance level is  $p < 0.05$  and there is no statistically significant difference, respectively. The  $n_{\text{sample}}$  in Figures (a) and (b) are 54, respectively.

## 4 Discussion

### 4.1 The mechanism underlying for the dimensions of deep-layer soil desiccation

Although DSM ( $>200$  cm) declined as the planted trees aged, and even reached the lowest limitation, shallow soil moisture ( $<200$  cm) remained stable (Figs. 2 and 4). This is attributed to the strong effect of rainfall and evapotranspiration on shallow soil moisture. However, DSM is often in a negative balance, being depleted by deep-rooted trees and unable to recover for a long time (Fang et al., 2016; Gao et al., 2020). As the critical water resource for plants to cope with extreme droughts, DSM of various sites was exhausted to the lowest limitation, posing a serious threat to the sustainability of tree growth under future climate conditions.

In our study, the lowest DSMD varied around  $-0.6$  regardless of tree species and site (Fig. 4). This challenges the assumption that moisture limitation of deep-layer soil desiccation is dependent on tree species. Based on the results of this study and opinions from the literature, Fig. 8 shows the mechanism by which plants regulate the moisture limitation of deep-layer soil desiccation. Soil water potential, when the soil hydraulic conductivity ( $K_s$ ) drops to lower values than the root hydraulic conductivity ( $K_r$ ), can be regarded as the critical soil matric potential, at which the soil begins to limit the water flux in the soil-plant continuum (Fig. 8; Cai et al., 2022). Thus, the soil with coarser texture has higher  $K_s$  when soil starts limiting tree's RWU. Correspondingly, the  $K_r$  value is higher in areas with less rainfall, which may be maintained by allocating more biomass to fine roots than that in areas with more rainfall (Fig. S5). In addition,  $VPD$  in the areas with less rainfall is relatively high, and the transpiration traction force increases (Will et al., 2013; Hayat et al., 2019), causing a larger water potential gradient between roots and leaves under the same soil moisture, and thus enabling roots to absorb more moisture. Therefore, although the physiological and growth characteristics of *M. pumila* and *R. pseudoacacia* across different sites were markedly different



(Table 2; Fig. 7; Fig. S5), the lowest DSMD of all tree species at each site fluctuated around -0.6. This indicates that the amount of soil moisture absorbed by plants is determined by *VPD* and soil water availability, which is mainly affected by the precipitation and soil structure (Wu et al., 2015). Notably, the lowest DSMD was very close to the DSMD value corresponding to the local *PWP*, regardless of tree species (Fig. 4). This might be attributed to different plant species wilted at similar water contents in soils with low clay content (Torres et al., 2021). Overall, our study confirms that *PWP* is a reliable indicator of the moisture limitation of deep-layer soil desiccation for the tree species examined. These findings provide important information for the sustainable development of plantations on the LOP.

When soil water in the profile becomes limited, plants extend their roots into the deep soil to expand their water-hunting range during the dry season (Fig. 8; Ivanov et al., 2012). Our results showed that for the sampled trees, the maximum RWU depth reached 18.0-22.0 m for *M. pumila* orchards across different sites, and 18.4-18.8 m for *R. pseudoacacia* forests in Changwu and Yan'an, while in Mizhi it was more than 25 m (Fig. 5). These depth ranges are similar to the maximum RWU depth of the artificial *Caragana microphylla* forest reported by Wang et al. (2009). Divergence in the maximum RWU depth of the same tree species examined at different sites was mainly due to trees adopting different biomass allocation strategies to adapt to varying drought aridity (Mayoral et al., 2016; Valverdi et al., 2019; Zhao et al., 2022). This was evident as the fine root dry weight density distributed at greater soil depth for *R. pseudoacacia* plantation examined in Mizhi than that in Changwu and Yan'an (Fig. S5), while the plant height of *R. pseudoacacia* trees in Mizhi was lower than that in Changwu and Yan'an (Table 2). Due to the longer flow path, the greater hydraulic resistance for upward water transfer (Mencuccini, 2003; Zwieniecki et al., 2003), *R. pseudoacacia* trees examined in Changwu and Yan'an were taller, which made it relatively difficult for them to absorb water from deeper soil layers. In contrast, due to substantial human intervention such as regular canopy pruning in every early spring during periods, the maximum RWU depth of *M. pumila* plantations across different sites both were between 18.0-22.0 m. This difference between tree species was consistent with the hypothesis. In addition to human management factors, the difference in the maximum RWU depth examined for *M. pumila* and *R. pseudoacacia* in Mizhi was in that, the early-stage water consumption of the latter is higher (Wu et al., 2021), leading to lower deep soil moisture (>2 m) across different sites than *M. pumila* plantations (Fig. S3). Furthermore, the larger *VPD* and the coarser soil texture (Fig. 8) helped *R. pseudoacacia* trees to absorb water by growing deeper roots (>25 m) in this site. Although the maximum RWU depth of *R. pseudoacacia* trees in Mizhi exceeded the measurement depth, the findings from both field observation (Li et al., 2019) and model simulation (Li et al., 2022) indicated that plantations faced challenges in extracting substantial amounts of water from deep soil due to deep-layer soil desiccation. Instead, they primarily rely on shallow soil water replenished by rainfall. Therefore, the low precipitation exacerbates the drought stress for plantations in semi-arid region, considering the projected increase in both the intensity and duration of future drought events (Miller et al., 2023).

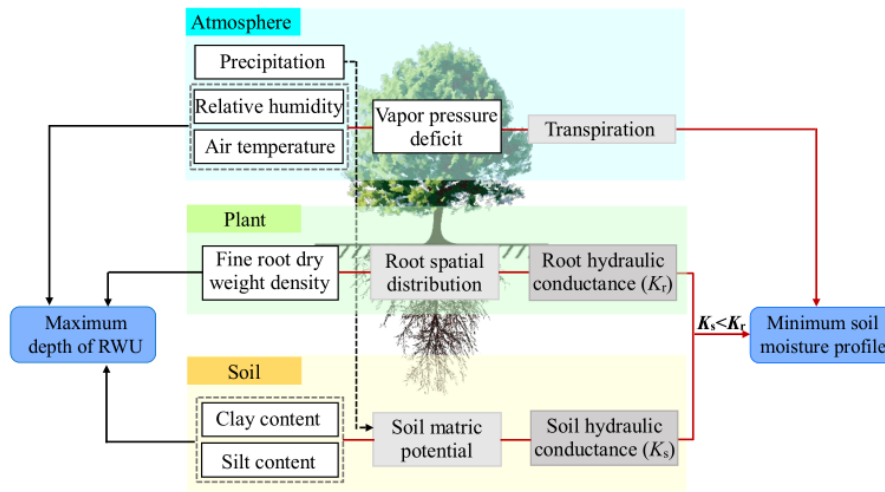


**Figure 8:** Regulatory mechanism of the extreme influence of root water uptake (RWU) on deep soil moisture based on literature and field measured data. The parameters of soil-plant-atmosphere continuum (SPAC) in the white rectangle are quantized, the gray rectangle represents the intermediate variables that the parameters of SPAC cause the result of minimum soil moisture profile (moisture limitation), the blue rounded rectangle represents the moisture limitation and the maximum RWU depth. The red arrow, the black solid arrow and the black dotted arrow indicate that the parameters of SPAC have a significant ( $p < 0.05$ ) effect on the moisture limitation, have an influence on the maximum RWU depth, and have an indirect effect on two results, respectively.

## 4.2 Variations of the hydraulic conductivity of plantations

The result revealed that branch xylem of similar aged trees suffered embolism to different degrees in the plantations sampled in this study (Fig. 7). This was consistent with the hypothesis that the xylem hydraulic conductivity of the planted trees varied among tree species and sites. The variation of *NPLC* across different sites can be mainly attributed to the degree of deep soil desiccation as well as probably the disparities in shallow soil moisture influenced by precipitation. Dried soil seriously limited the process of RWU, and water absorption of trees was difficult to meet the needs of transpiration, resulting in the leaf stomata closing to prevent excessive reduction of leaf water potential (Yang et al., 2022). Subsequently, the water column in the xylem vessels was interrupted as the soil moisture availability decreased continuously (McDowell et al., 2018), and thus *NPLC* increased during prolonged dry periods (McDowell et al., 2018). Even though DSM of all sites was depleted to close to the local *PWP*, *NPLC* differed greatly between different climatic regions (Fig. 7) mainly due to the difference in precipitation. This suggests that the decrease in xylem hydraulic conductivity caused by the deep-layer soil desiccation may be restored after entering the rainy season for the studied plantations in Changwu and Yan'an. The *NPLC* of *R. pseudoacacia* trees in Mizhi, however, was significantly ( $p < 0.05$ , Fig. 7(b)) higher than that of other regions, which confirmed that even if the water absorption range was deeper, it could not buffer the negative effects of limited precipitation and extremely dry soil moisture profile on water transport in tree bodies. Therefore, the embolism in the conduit accumulated continuously as the water pool became exhausted, causing the severe and large-scale canopy die-back (Fig. S4; Arend et al., 2021). It should be noted that the *NPLC* value of *R. pseudoacacia* plantation might be higher due to the sample length (3-5 cm) in the XYL'EM measurement being shorter than the maximum vessel length, but the result was consistent with trees with most, or all, of their foliage dead exhibiting high rates of native embolism (78–100%) (Nolan et al., 2021). However, although the *NPLC* of *M. pumila* trees in

Mizhi was also high (Fig. 7(a)), there was no significant degradation in the plantation, and this interspecific difference might be mainly due to differences in tree height (Table 2) and the capacitance within their tissues and water loss (McDowell et al., 2022). The results indicate that mature (>24 year) *R. pseudoacacia* plantations on the LOP are already facing a great risk of dieback and even death in semi-arid regions similar to Mizhi.

### 4.3 Limitations and practical implications

Sampling the same tree species in different sites does not guarantee the same tree age due to objective factors such as differences in the time of planting and vegetation succession. Moreover, collecting large amounts of DSM data demands a great deal of resources, and the number of samples available in this study is limited. Therefore, the results of this study need to be verified in-depth across different tree ages and sites to guide vegetation management under local conditions.

Large numbers of tree deaths caused by prolonged drought are of great concern because trees play a critical ecological role and have the largest biomass and carbon storage (Feng et al., 2016; Bai et al., 2021). Hence, it is essential to understand the moisture limitation and the maximum RWU depth to maintain the sustainability of vegetation restoration under future climatic drying. Our study demonstrated that, except for *R. pseudoacacia* plantation in Mizhi, the 24-28-year-old *M. pumila* and *R. pseudoacacia* plantations sampled in this study reached both the soil moisture limitation and the maximum RWU depth across different sites; and the maximum DSMD was about -0.6, which corresponds to the DSMD at local *PWP*, regardless of tree species and site. This verifies that *PWP* is a reliable indicator of the moisture limitation of deep-layer soil desiccation for the tree species examined. When the precise wilting point of deep soil in different sites is difficult to determine, the lowest DSMD (-0.6) can be used as an index to judge whether DSM can sustain the survival of the typical plantations on the LOP during prolonged drought. Furthermore, the maximum RWU depth of the trees varied between sites in the plantations where soils were sampled. This suggests that the impact of water absorption by tree's root on soil hydrological processes and groundwater recharge is dependent on sites and tree species. Moreover, the trees suffered serious embolism with varying degrees were dependent on tree species and sites of the plantations sampled in this study. Consequently, plantations of 24 years and above face the greatest risk of dieback and death in drought years or prolonged dry periods, especially in semi-arid regions. The results provide practical insights into the sustainable development of vegetation restoration on the LOP under future extreme climate conditions.

## 5 Conclusions

Deep soil moisture (DSM) is crucial for the survival of deep-rooted plantations on the water-limited Loess Plateau, especially during prolonged dry periods. Our results revealed that the lowest deep soil moisture deficit was close to the soil moisture deficit at the permanent wilting point (*PWP*), regardless of tree species and site. This confirms that *PWP* is a reliable indicator

of the moisture limitation of deep soil desiccation for *M. pumila* and *R. pseudoacacia* trees. The corresponding water consumption depth reached 18.0-22.0 m for *M. pumila* orchards at different sites, and 18.4-18.8 m for *R. pseudoacacia* forests in Changwu and Yan'an, whereas it exceeded 25 m in the drier site of Mizhi, which depended largely on the availability of DSM and the ability of deep roots to transport water. Moreover, the native percentage loss of hydraulic conductivity of the branches of planted trees varied from 74.9% to 96.5% in the plantations sampled in this study, and exhibited distinct differences between tree species and sites, suggesting that dieback and tree mortality might occur. Our study provides insights into the management and sustainable development of revegetated sites in the water-limited regions including the Loess Plateau.

## Data availability

The basic data, including extracted and measured set of soil moisture, environmental factors, and percentage loss of hydraulic conductivity of trees' branches, are available for download at <https://doi.org/10.5281/zenodo.7412472>.

## Author contributions

XG and XZ conceived the study; NH, DG, YW and DG performed field experiments and collected the data; NH performed the analysis and prepared the first draft of the manuscript with the help of LT and LZ; XG edited and commented on the manuscript.

## Competing interests

The authors declare that they have no conflict of interest.

## Acknowledgments

The authors thank Shaofei Wang and Min Yang for their help. This work was jointly supported by the National Natural Science Foundation of China (42125705), Natural Science Basic Research Program of Shaanxi Province (2021JC-19), the Cyrus Tang Foundation, the Shaanxi Key Research and Development Program (2020ZDLNY07-04), Shaanxi Province Key R&D Plan (2022NY-064) and Chinese Universities Scientific Fund (2452020242).

## References

Araújo, C. S. P. de, Silva, I. A. C., Ippolito, M., and Almeida, C. D. G. C. de: Evaluation of air temperature estimated by ERA5-Land reanalysis using surface data in Pernambuco, Brazil. *Environ. Monit. Assess*, 194, 381-394, <https://doi.org/10.1007/s10661-022-10047-2>, 2022.

- Arend, M., Link, R. M., Patthey, R., Hoch, G., Schuldt, B., and Kahmen, A.: Rapid hydraulic collapse as cause of drought-induced mortality in conifers, *PNAS*, 118(16), <https://doi.org/10.1073/pnas.2025251118>, 2021.
- Cao, S., Xia, C., Suo, X., Wei Z.: A framework for calculating the net benefits of ecological restoration programs in China, *Ecosyst. Serv.*, 50(2021), 101325, <https://doi.org/10.1016/j.ecoser.2021.101325>, 2021.
- 490 Choat B., Brodribb T. J., Brodersen C. R., Duursma R. A., López R., and Medlyn B. E.: Triggers of tree mortality under drought, *Nature*, 558, 531–539, <https://doi.org/10.1038/s41586-018-0240-x>, 2018.
- Bai, X., Jia, X., Zhao, C., and Shao, M.: Artificial forest conversion into grassland alleviates deep-soil desiccation in typical grass zone on China's Loess Plateau: Regional modeling, *Agric. Ecosyst. Environ.*, 320 (5), 107608, <https://doi.org/10.1016/j.agee.2021.107608>, 2021.
- 495 Balland, V., Pollacco, J., and Arp, P.: Modeling soil hydraulic properties for a wide range of soil conditions. *Ecol. Model.*, 219 (3-4), 300-316, <https://doi.org/10.1016/j.ecolmodel.2008.07.009>, 2008.
- Breshears, D. D., Adams, H. D., Eamus, D., McDowell, N. G., Law, D. J., Will, R. E., Williams, A. P., and Zou, C. B.: The critical amplifying role of increasing atmospheric moisture demand on tree mortality and associated regional die-off, *Front. plant sci.*, 4, 266-269, <https://doi.org/10.3389/fpls.2013.00266>, 2013.
- 500 Cai, G., Ahmed, M. A., Abdalla, M., and Carminati, A.: Root hydraulic phenotypes impacting water uptake in drying soils, *Plant cell environ.*, 45 (3), 650-663, <https://doi.org/10.1111/pce.14259>, 2022.
- Deng L., Yan W., Zhang Y., and Shanguan Z.: Severe depletion of soil moisture following land-use changes for ecological restoration: Evidence from northern China, *For. Ecol. Manage.*, 366, 1-10, <https://doi.org/10.1016/j.foreco.2016.01.026>, 2016.
- 505 Fang, X., Zhao, W., Wang, L., Feng, Q., Ding, J., Liu, Y., and Zhang, X.: Variations of deep soil moisture under different vegetation types and influencing factors in a watershed of the Loess Plateau, China, *Hydrol. Earth Syst. Sci.*, 20 (8), 3309-3323, <https://doi.org/10.5194/hess-20-3309-2016>, 2016.
- Feng, X., Fu, B., Piao, S., Wang, S., Ciais, P., Zeng, Z., Lü Y., Zeng Y., Li Y., Jiang X., and Wu B.: Revegetation in China's Loess Plateau is approaching sustainable water resource limits, *Nat. Clim. Change*, 6 (11), 1019-1022, [10.1038/nclimate3092](https://doi.org/10.1038/nclimate3092), 2016.
- 510 Fu, B., Wang, S., Liu, Y., Liang, W., and Miao, C.Y.: Hydrogeomorphic ecosystem responses to natural and anthropogenic changes in the Loess Plateau of China, *Annu. Rev. Earth Planet Sci.*, 45, 223-243, <https://doi.org/10.1146/annurev-earth-063016-020552>, 2016.
- Fuchs, S., Leuschner, C., Link M. R., and Schuldt, B.: Hydraulic variability of three temperate broadleaf tree species along a water availability gradient in central Europe, *New Phytol.*, 231 (4), 1387-1400, <https://doi.org/10.1111/nph.17448>, 2021.
- 515 Fu, X., Shao, M., Wei, X., and Horton, R.: Soil organic carbon and total nitrogen as affected by vegetation types in Northern Loess Plateau of China. *Geoderma*, 155 (1-2), 31-35, <https://doi.org/10.1016/j.geoderma.2009.11.020>, 2010.

- Gao, X., Wu, P., Zhao, X., Wang, J., Shi, Y.: Effects of land use on soil moisture variations in a semi-arid catchment: Implications for land and agricultural water management, *Land Degrad. Develop.*, 25, 163-172, <https://doi.org/10.1002/ldr.1156>, 2014.
- 520 Gao, X., Li, H., Zhao, X., Ma, W., and Wu, P.: Identifying a suitable revegetation technique for soil restoration on water-limited and degraded land: Considering both deep soil moisture deficit and soil organic carbon sequestration, *Geoderma*, 319 (5), 61-69, <https://doi.org/10.1016/j.geoderma.2018.01.003>, 2018.
- Gao, X., Zhao, X., Wu, P., Yang, M., Ye, M., Tian, L., Zou Y., Wu Y., Zhang F., and Siddique K. H. M.: The economic-environmental trade-off of growing apple trees in the drylands of China: A conceptual framework for sustainable intensification, *J. Clean. Prod.*, 296 (3), 126497, <https://doi.org/10.1016/j.jclepro.2021.126497>, 2021.
- 525 Gao, X., Li, H., and Zhao, X.: Impact of land management practices on water use strategy for a dryland tree plantation and subsequent responses to drought, *Land Degrad Dev*, 32, 439-452, <https://doi.org/10.1002/ldr.3687>, 2020.
- Gao, X., He, N., Jia, R., Hu, P., Zhao, X.: Redesign of dryland apple orchards by intercropping the bioenergy crop canola (*Brassica napus* L.): Achieving sustainable intensification, *Glob. Change Biol. Bioenergy*, 14, 378-392, <https://doi.org/10.1111/gcbb.12916>, 2022.
- 530 Gauthey, A., Peters, J.M.R., Lòpez, R., Carins-Murphy, M.R., Carins-Murphy, C.M., Tissue, D.T., Medlyn, B.E., Brodribb, T.J., Choat, B.: Mechanisms of xylem hydraulic recovery after drought in *Eucalyptus saligna*, *Plant Cell Environ.*, 45, 1216–1228, <https://doi.org/10.1111/pce.14265>, 2022.
- Gessler, A., Bottero, A., Marshall, J., Arend M.: The way back: recovery of trees from drought and its implication for acclimation, *New Phytol.*, 228(6), 1704-1709, <https://doi.org/10.1111/nph.16703>, 2020.
- 535 Griscom, B., Jackson, R. B., Konijnendijk, C., Luysaert, S., Friess, D., Rudee, A., and Seddon, N.: Trees as Nature-Based Solutions, *One earth*, 2, 387-389, 2020.
- Hayat, F., Ahmed, M. A., Zarebanadkouki, M., Cai, G., and Carminati, A.: Measurements and simulation of leaf xylem water potential and root water uptake in heterogeneous soil water contents, *Adv. Water Resour.*, 124, 96–105, <https://doi.org/10.1016/j.advwatres.2018.12.009>, 2019.
- 540 Hou, Q., Huang X., Han, S., Zhang, X.: The status of soil moistures and nutrients in small-old-tree stands and impact on tree growth (In Chinese), 5(2), 75-83, *Journal of Soil Water Conservation*, <https://doi.org/10.13870/j.cnki.stbcbx.1991.02.012>, 1991.
- Ivanov, V. Y., Hutrya, L. R., Wofsy, S. C., Munger, J. W., Saleska, S. R., Oliveira, R. C. de, and Camargo, P. B.: Root niche separation can explain avoidance of seasonal drought stress and vulnerability of overstory trees to extended drought in a mature Amazonian forest, *Water Resour. Res.*, 48 (12), 12507, <https://doi.org/10.1029/2012WR011972>, 2012.
- 545 Jia, X., Shao, M., Zhu, Y., and Luo, Y.: Soil moisture decline due to afforestation across the Loess Plateau, China, *J. Hydrol.*,

546, 113-122, <https://doi.org/10.1016/j.jhydrol.2017.01.011>, 2017.

Jia, X., Shao, M., Wei, X., Zhu, Y., Wang, Y., and Hu, W.: Policy development for sustainable soil water use on China's Loess Plateau, *Sci. Bull.*, 65, 2053-2056, <https://doi.org/10.1016/j.scib.2020.09.006>, 2020.

550

Li, B., Li, P., Zhang, W., Ji, J., Liu, G., and Xu, M.: Deep soil moisture limits the sustainable vegetation restoration in arid and semi-arid Loess Plateau, *Geoderma*, 399 (12), 115122, <https://doi.org/10.1016/j.geoderma.2021.115122>, 2021a.

Li, B., Zhang W., Li S., Wang J., Liu G., and Xu M.: Severe depletion of available deep soil water induced by revegetation on the arid and semiarid Loess Plateau, *For. Ecol. Manage.*, 491, 119156, <https://doi.org/10.1016/j.foreco.2021.119156>, 2021b.

555

Li, H., Ma, X., Lu, Y., Ren, R., Cui, B., and Si, B.: Growing deep roots has opposing impacts on the transpiration of apple trees planted in subhumid loess region, *Agric. Water Manage.*, 258, 107207, <https://doi.org/10.1016/j.agwat.2021.107207>, 2021.

Li, H., Luo, Y., Sun, L., Li, X., Ma, C., Wang, X., Jiang, T., Zhu, H.: Modelling the artificial forest (*Robinia pseudoacacia* L.) root–soil water interactions in the Loess Plateau, China, *Hydrol. Earth Syst. Sci.*, 26, 17-34, <https://doi.org/10.5194/hess-26-17-2022>, 2022.

560

Li, H., Si, B., Wu, P., and McDonnell, J.: Water mining from the deep critical zone by apple trees growing on loess, *Hydrol. Process*, 33, 320-327, <https://doi.org/10.1002/hyp.13346>, 2019.

Liu, Y., Kumar, M., Katul, G. G., Feng, X., and Konings, A. G.: Plant hydraulics accentuates the effect of atmospheric moisture stress on transpiration, *Nat. Clim. Change*, 10 (7), 691-695, <https://doi.org/10.1038/s41558-020-0781-5>, 2020.

565

Lucia H. W., Neyde F. B. G., Renato P. de L., Cassio A. T., Lorena C. T., and Ariane L. de P.: Comparing the classical permanent wilting point concept of soil (–15, 000 hPa) to biological wilting of wheat and barley plants under contrasting soil textures, *Agric. Water Manage.*, 230, 105965, <https://doi.org/10.1016/j.agwat.2019.105965>, 2020.

Mayoral C., Pardos M., Sánchez-González M., Brendel O., Pita P.: Ecological implications of different water use strategies in three coexisting mediterranean tree species, *For. Ecol. Manage.*, 382, 76–87, <https://doi.org/10.1016/j.foreco.2016.10.002>, 2016.

570

McDowell, N., Allen, C. D., Anderson-Teixeira, K., Brando, P., Brien, R., Chambers, J., Christoffersen, B., Davies, S., Doughty, C., Duque, A., Espirito-Santo, F., Fisher, R., Fontes, C. G., Galbraith, D., and Goodsman, D.: Drivers and mechanisms of tree mortality in moist tropical forests, *New Phytol.*, 219 (3), 851-869, <https://doi.org/10.1111/nph.15027>, 2018.

575

McDowell, N.G., Sapes, G., Pivovarov, A., Adams, H.D., Allen, C.D., Anderegg, W.R.L., Arend, M., Breshears, D.D., Brodrick, T., Choat, B., Cochard, H., et al.: Mechanisms of woody-plant mortality under rising drought, CO<sub>2</sub> and vapour pressure deficit, *Nat. Rev. Earth Env.*, 3(5), 294-308, <https://doi.org/10.1038/s43017-022-00272-1>, 2022.

- Mencuccini M.: The ecological significance of long-distance water transport: short-term regulation, long-term acclimation and the hydraulic costs of stature across plant life forms, *Plant Cell Environ.*, 26,163–182, <https://doi.org/10.1046/j.1365-3040.2003.00991.x>, 2003.
- 580
- Miller, D.L., Wolf, S., Fisher, J.B., Zaitchik, B.F., Xiao, J.F., Keenan, T.F.: Increased photosynthesis during spring drought in energy-limited ecosystems, *Nat. Commun.*, 14, 7828, <https://doi.org/10.1038/s41467-023-43430-9>, 2023.
- Mokany, K., Raison, R. J., and Prokushkin, A. S.: Critical analysis of root: shoot ratios in terrestrial biomes, *Global Change Biol.*, 12, 84-96, <https://doi.org/10.1111/j.1365-2486.2005.001043.x>, 2005.
- 585
- Schuldt, B., Knutzen, F., Delzon, S., Jansen, S., Mueller-Haubold, H., Burlett, R., Clough, Y., and Leuschner, C.: How adaptable is the hydraulic system of European beech in the face of climate change-related precipitation reduction? *New Phytol.*, 210, 443–458, <https://doi.org/10.1111/nph.13798>, 2016.
- Shao, M., Wang, Y., Xia, Y., and Jia, X.: Soil Drought and Water Carrying Capacity for Vegetation in the Critical Zone of the Loess Plateau: A Review, *Vadose Zone J.*, 17, 170077, <https://doi.org/10.2136/vzj2017.04.007>, 2018.
- 590
- Shi, P., Huang, Y., Ji, W., Xiang, W., Evaristo, J., and Li, Z.: Impacts of deep-rooted fruit trees on recharge of deep soil water using stable and radioactive isotopes, *Agr. Forest Meteorol.*, 300 (23), 108325, <https://doi.org/10.1016/j.agrformet.2021.108325>, 2021.
- Stojnic, S., Suchocka, M., Benito-Garzón, M., Torres-Ruiz, J.M., Cochard, H., Bolte, A., Coccozza, C., Cvjetkovic´, B., de Luis, M., Martinez-Vilalta, J., Ræbild, A., Tognetti, R., and Delzon, S.: Variation in xylem vulnerability to embolism in European beech from geographically marginal populations, *Tree Physiol.*, 38, 173-185, <https://doi.org/10.1093/treephys/tpx128>, 2017.
- 595
- Stovall, A. E. L., Shugart, H., and Yang, X.: Tree height explains mortality risk during an intense drought, *Nat. Commun.*, 10 (1), 4385, <https://doi.org/10.1038/s41467-019-12380-6>, 2019.
- 600
- Su, B. and Shangguan, Z.: Decline in soil moisture due to vegetation restoration on the Loess Plateau of China, *Land Degrad. Dev.*, 30 (3), 290-299, <https://doi.org/10.1002/ldr.3223>, 2019.
- Tao, Z., Li, H., and Si, B.: Stand age and precipitation affect deep soil water depletion of economical forest in the loess area, *Agr. Forest Meteorol.*, 310, 108636, <https://doi.org/10.1016/j.agrformet.2021.108636>, 2021.
- Tormena, C., Karlen, D. L., Logsdon, S., and Cherubin, M. R.: Corn stover harvest and tillage impacts on near-surface soil physical quality, *Soil Till. Res.*, 166, 122-130, <https://doi.org/10.1016/j.still.2016.09.015>, 2017.
- 605
- Torres, L. C., Keller T., Lima R. P. de, Tormena, C. A., Lima H. V. de, and Giarola N. F. B.: Impacts of soil type and crop species on permanent wilting of plants, *Geoderma*, 384, 114798, <https://doi.org/10.1016/j.geoderma.2020.114798>, 2021.
- Valverdi NA., Cheng L., Kalcsits L.: Apple scion and rootstock contribute to nutrient uptake and partitioning under different belowground environments, *Agron. J.*, 9(8), 415, <https://doi.org/10.3390/agronomy9080415>, 2019.



- 610 Wang, L., Wang, Q., Wei, S., Shao, M., and Li, Y.: Soil desiccation for Loess soils on natural and regrown areas, *For. Ecol. Manage.*, 255 (7), 2467-2477, <https://doi.org/10.1016/j.foreco.2008.01.006>, 2008.
- Wang, S., Gao, X., Yang, M., Huo, G., Song, X., Siddique, K.H.M., Wu, P., and Zhao, X.: The natural abundance of stable water isotopes method may overestimate deep-layer soil water use by trees, *Hydrol. Earth Syst. Sci.*, 27, 123–137, <https://doi.org/10.5194/hess-27-123-2023>, 2023.
- 615 Wang, Y., Shao, M., and Liu, Z.: Large-scale spatial variability of dried soil layers and related factors across the entire Loess Plateau of China, *Geoderma*, 159, 99-108, <https://doi.org/10.1016/j.geoderma.2010.07.001>, 2010.
- Wang, Y., Shao, M., and Liu, Z.: Pedotransfer functions for predicting soil hydraulic properties of the Chinese Loess Plateau. *Soil Sci.*, 177 (7), 424-432, <https://doi.org/10.1097/SS.0b013e318255a449>, 2012.
- Wang, Y., Shao, M., Zhu, Y., and Liu, Z.: Impacts of land use and plant characteristics on dried soil layers in different climatic  
620 regions on the Loess Plateau of China, *Agr. Forest Meteorol.*, 151 (4), 437-448, <https://doi.org/10.1016/j.agrformet.2010.11.016>, 2011.
- Wang, Z., Liu, B., Liu, G., and Zhang, Y.: Soil water depletion depth by planted vegetation on the Loess Plateau, *Sci. China Ser D-Earth Sci*, 52(6), 835-842, <https://doi.org/10.1007/s11430-009-0087-y>, 2009.
- Will, R. E., Wilson, S. M. Zou, C. B., and Hennessey, T. C.: Increased vapor pressure deficit due to higher temperature leads  
625 to greater transpiration and faster mortality during drought for tree seedlings common to the forest-grassland ecotone, *New Phytol.*, 200 (2), 366-374, <https://doi.org/10.1111/nph.12321>, 2013.
- Wu, W., Li, H., Feng, H., Si, B., Chen, G., Meng, T., Li, Y., and Siddique, K. H. M.: Precipitation dominates the transpiration of both the economic forest (*Malus pumila*) and ecological forest (*Robinia pseudoacacia*) on the Loess Plateau after about  
630 15 years of water depletion in deep soil, *Agr. Forest Meteorol.*, 297 (1–4), 108244, <https://doi.org/10.1016/j.agrformet.2020.108244>, 2021.
- Wu, Y., Huang, M., Warrington, D.: Black Locust Transpiration Responses to Soil Water Availability as Affected by Meteorological Factors and Soil Texture, *Pedosphere*, 25(1), 57-71, [https://doi.org/10.1016/S1002-0160\(14\)60076-X](https://doi.org/10.1016/S1002-0160(14)60076-X), 2015.
- Yang, M., Gao, X., Wang, S., and Zhao, X.: Quantifying the importance of deep root water uptake for apple trees' hydrological  
635 and physiological performance in drylands, *J. Hydrol.*, 606 (11), 127471, <https://doi.org/10.1016/j.jhydrol.2022.127471>, 2022.
- Zhao, L., He, N., Wang, J., Siddique, K. H. M., Gao, X., and Zhao, X.: Plasticity of root traits in a seedling apple intercropping system driven by drought stress on the Loess Plateau of China, *Plant Soil*, 24 (1), 273, <https://doi.org/10.1007/s11104-022-05603-1>, 2022.
- 640 Zhu, G., Deng, L., Zhang, X., Shangguan, Z.: Effects of grazing exclusion on plant community and soil physicochemical

properties in a desert steppe on the Loess Plateau, China, *Ecol. Eng.*, 90, 372-381, <https://doi.org/10.1016/j.ecoleng.2016.02.001>, 2016.

Zhu, X.: Rebuild soil reservoir is a rational approach for soil and water conservation on the Loess Plateau (In Chinese), *Bulletin of Chinese Academy of Sciences*, 21(4), 320-324, <https://doi.org/10.16418/j.issn.1000-3045.2006.04.014>, 2006.

645 Zhu, X.: Rescue the “soil reservoir” to control the ecological environment of the Loess Plateau (In Chinese), *Bulletin of Chinese Academy of Sciences*, 2000(04), 293-295, <https://doi.org/10.16418/j.issn.1000-3045.2000.04.019>, 2000.

Zwieniecki, M. A., Thompson, M. V., & Holbrook, N. M.: Understanding the Hydraulics of Porous Pipes: Tradeoffs Between Water Uptake and Root Length Utilization, *J. Plant Growth Regul.*, 21(4), 315–323, <https://doi.org/10.1007/s00344-003-0008-9>, 2003.